Candidate genes for shell colour polymorphism in *Cepaea nemoralis*

Jesse Kerkvliet Corresp., [1] , **Tjalf de Boer** [2, 3] , **Menno Schilthuizen** [4] , **Ken Kraaijeveld** [3, 5]

[1] Bio-informatics, University of Applied Sciences Leiden, Leiden, The Netherlands

[2] MicroLife Solutions, Amsterdam, The Netherlands

[3] Department of Ecological Sciences, Vrije Universiteit Amsterdam, Amsterdam, The Netherlands

[4] Naturalis Biodiversity Center, Leiden, The Netherlands

[5] Leiden Genome Technology Center, Leiden University Medical Center, Leiden, The Netherlands

Corresponding Author: Jesse Kerkvliet
Email address: jesse@kerkvliet.info

The characteristic ground colour and banding patterns on shells of the land snail *Cepaea nemoralis* form a classic study system for genetics and adaptation as it varies widely between individuals. We use RNAseq analysis to identify candidate genes underlying this polymorphism. We sequenced cDNA from the foot and the mantle (the shell-producing tissue) of four individuals of two phenotypes and produced a *de novo* transcriptome of 147,397 contigs. Differential expression analysis identified a set of 1,961 transcripts that were upregulated in mantle tissue. Sequence variant analysis resulted in a set of 2,592 transcripts with single nucleotide polymorphisms (SNPs) that differed consistently between the phenotypes. Inspection of the overlap between the differential expression analysis and SNP analysis yielded a set of 197 candidate transcripts, of which 38 were annotated. Four of these transcripts are thought to be involved in production of the shell's nacreous layer. Comparison with morph-associated Restriction-site Associated DNA (RAD)-tags from a published study yielded eight transcripts that were annotated as metallothionein, a protein that is thought to inhibit the production of melanin in melanocytes. These results thus provide an excellent starting point for the elucidation of the genetic regulation of the *Cepaea nemoralis* shell colour polymorphism.

Candidate genes for shell colour polymorphism in *Cepaea nemoralis*

Jesse Kerkvliet[1], Tjalf de Boer[2,3], Menno Schilthuizen[4], Ken Kraaijeveld[2,5]

[1]Bioinformatics, University of Applied Sciences Leiden, Leiden, The Netherlands

[2]Department of Ecological Sciences, Vrije Universiteit Amsterdam, Amsterdam, The Netherlands

[3] MicroLife Solutions, Amsterdam, The Netherlands

[4]Naturalis Biodiversity Center, Leiden, the Netherlands

[5]Leiden Genome Technology Center, Leiden University Medical Center, Leiden, The Netherlands

Corresponding author: Jesse Kerkvliet, Jesse@Kerkvliet.info

Abstract

The characteristic ground colour and banding patterns on shells of the land snail *Cepaea nemoralis* form a classic study system for genetics and adaptation as it varies widely between individuals. We use RNAseq analysis to identify candidate genes underlying this polymorphism. We sequenced cDNA from the foot and the mantle (the shell-producing tissue) of four individuals of two phenotypes and produced a *de novo* transcriptome of 147,397 contigs. Differential expression analysis identified a set of 1,961 transcripts that were upregulated in mantle tissue. Sequence variant analysis resulted in a set of 2,592 transcripts with single nucleotide polymorphisms (SNPs) that differed consistently between the phenotypes. Inspection of the overlap between the differential expression analysis and SNP analysis yielded a set of 197 candidate transcripts, of which 38 were annotated. Four of these transcripts are thought to be involved in production of the shell's nacreous layer. Comparison with morph-associated Restriction-site Associated DNA (RAD)-tags from a published study yielded eight transcripts that were annotated as metallothionein, a protein that is thought to inhibit the production of melanin in melanocytes. These results thus provide an excellent starting point for the elucidation of the genetic regulation of the *Cepaea nemoralis* shell colour polymorphism.

Introduction

Since the first studies of selection on the banding patterns and colours on the shell of the land snail *Cepaea nemoralis* over 60 years ago (Cain & Sheppard, 1950, 1952, 1954), the polymorphism has become a classic study system for genetics and adaptation (Jones, Leith & Rawlings, 1977; Cook, 1998; Silvertown et al., 2011; Cameron & Cook, 2012). For example, shell colour affects habitat-dependent predation risk and thermoregulation (Lamotte, 1959; Clarke, 1962; Arnold, 1971; Greenwood, 1974). More recently, the *Cepaea* shell colour polymorphism became the subject of the citizen science project Evolution MegaLab, in which citizen scientists are asked to score the phenotypes of *Cepaea* snails in their surroundings and upload their records to the MegaLab website (Worthington et al., 2012). The aim of this project is to show that (possibly human-induced) selection differences can result in differences in allele frequencies on a local as well as a continental scale (Silvertown et al., 2011; Schilthuizen, 2013).

Despite the prominence of the *Cepaea* study system in scientific discourse as well as public outreach, little is known about the underlying molecular genetic machinery that produces the different phenotypes. The *Cepaea* shell polymorphism consists of nine phenotypic traits, which include shell ground colour and various aspects of the banding pattern (Richards et al., 2013). Genes underlying five of these traits are closely linked to form a so-called supergene (Schwander, Libbrecht & Keller, 2014), which inherit with very little recombination between the alleles, keeping the alleles together as one large gene. (Schwander, Libbrecht & Keller, 2014). Richards *et al.* (2013) identified eleven restriction-site associated DNA (RAD) tags that were linked to the supergene. Three of these tags were

within ~0.6cM of the supergene. Mann & Jackson (2014) characterized the major proteinaceous components of the *C. nemoralis* shell, but were unable to identify proteins associated with shell pigmentation. The aim of our work is to identify candidate genes that may underlie the *Cepaea* shell polymorphism.

To identify candidate genes that play a role in the polymorphism, the RNA of four juvenile *C. nemoralis* individuals (two brown/unbanded and two yellow/banded) was sequenced. For each individual, we sequenced the transcriptome of the mantle (the organ in which the shell is formed) and the snail foot. Since the polymorphism is only visible in the shell, we focus on candidate genes that are upregulated in the mantle. Within this set of mantle-specific genes, we search for sequence variants that differ consistently between different phenotypes. Furthermore, we search for the three supergene-associated RAD tags reported by (Richards et al., 2013), as they are found in near proximity of the supergene. Our results provide the first clues to the molecular mechanisms underlying the *Cepaea* polymorphism and will provide a starting point for elucidating the genetic architecture of this classic polymorphism.

Methods

Sample collection, mRNA extraction, sequencing and assembly

Four juvenile *C. nemoralis* with different phenotypes (two with brown shell and no banding and two with a yellow shell with multiple dark bands; Fig. S1) were collected at the Van Veldhuizenbos near Dronten, The Netherlands. Total RNA was extracted separately from the mantle and the foot for each of the four *C. nemoralis* individuals using the NucleoSpin

RNA kit (Macherey-Nagel), following the manufacturer's protocol. The remains of the specimens have been deposited in the alcohol collection of Naturalis Biodiversity Center under reference numbers RMNH.5004228-5004231. The total RNA was subjected to polyA selection, converted to cDNA and used to generate sequencing libraries as described in (Salazar-Jaramillo et al., 2017). The libraries were paired-end 2x100 bp sequenced on an Illumina HiSeq 2000 at the Leiden Genome Technology Center.

De novo assembly, protein prediction and annotation

Sequence reads of all eight samples were combined to create a reference transcriptome assembly using Trinity v2.0.5 with default settings (Grabherr et al., 2011). To reduce redundancy, transcripts were clustered using CD-HIT-Est (Fu et al., 2012) at a cut-off of 95% identity. To remove contamination, we used NCBI's VecScreen. This tool searches for segments that match sequences in the UniVec database. We used BUSCO (Simao et al., 2015) to assess the completeness of the transcriptome. This tool searches the transcriptome for a reference set of single-copy orthologs. The metazoan set (odb9) was used as a reference set. All genes in the transcriptome were annotated for gene ontology (GO) using the Trinotate part of the Trinity package. Trinotate uses blastp and blastx to compare the predicted peptide sequences and the reference transcriptome to the uniprot_sprot and the uniprot_uniref peptide databases, performs an hmm-scan on the Pfam-A database and assigns GO terms.

Differential expression

105 To identify genes that were overexpressed in the shell-forming mantle tissue, the Trinity
106 RNA-seq pipeline (Grabherr et al., 2011) was used. First, the reads for both organs in all
107 four individuals were mapped to the reference transcriptome. Second, the mapped reads
108 were counted to visualize the expression of these transcripts, using the estimation method
109 eXpress (Roberts & Pachter, 2013). A high count of mapped reads indicates a high
110 expression rate, while a low count of mapped reads indicates a low expression rate. With
111 the estimated counts of reads, expression profiles were generated using the R-package
112 EdgeR (Robinson, McCarthy & Smyth, 2010). Normalization took place as part of the EdgeR
113 workflow. The profiles were then filtered on fold change and false discovery rate (FDR)
114 with the Trinity default cut-off scores of 4 and 0.001 respectively. The genes that were
115 overexpressed in the mantle were selected for further analysis. A heatmap of differentially
116 expressed genes versus samples was produced using the script analyze_diff_expr.pl within
117 the Trinity package.
118
119 *Sequence variants*
120 To identify consistent sequence differences between the two phenotypes (yellow/banded
121 and the brown/unbanded), we conducted variant calling following the following protocol.
122 First, reads were mapped to the reference transcriptome using Bowtie2 (Langmead &
123 Salzberg, 2012). Next, GATK's HaplotypeCaller (McKenna et al., 2010) was run to search for
124 single-nucleotide polymorphisms (SNPs). The default parameters were used with a
125 stand_call confidence of 20.0 and a stand_emit confidence of 20.0. The VariantFiltration
126 tool was used with default parameters to filter out false-positive variants. Clusters were
127 generated when 3 SNPs were present within a window of 35 bases. Variants with a Fisher-

strand Score (FS) greater than 30.0 or a quality by depth (QD) value less than 2.0 were filtered out. SNPs with sequencing depth less than 10 in any of the samples were removed. The effect of each SNP on the transcript product was predicted using SnpEff (Cingolani et al., 2012).

The resulting set of SNPs was filtered for consistency with the phenotypes using GATK and custom R-scripts. The inheritance of the polymorphism is well understood (Cain & Sheppard, 1954; Murray, 1963; Jones, Leith & Rawlings, 1977). The brown ground colour is dominant over the yellow ground colour and absence of banding is dominant over the presence of multiple bands. The candidate SNPs were therefore filtered so that the brown, unbanded snails were either heterozygous or homozygous and the yellow, banded snails were homozygous. Mantle-enriched transcripts contained at least one phenotype-consistent sequence variant were blastn-searched (Altschul et al., 1990) against the non-redundant nucleotide database.

RAD-tags

Richards *et al.* (2013) identified eleven anonymous RAD tag sequences that lie near the colour-polymorphism supergene. In the original research, a cut-off of 96 base pairs was used for the tags. Because of this, the tags are shorter than the full assembly of the RAD tag reads. The overlapping parts of the RAD tag reads were used to generate a consensus for each tag that was longer than the original consensus RAD tag. These extended tags were blast-searched against the reference transcriptome using the megablast algorithm within the Blast+ (Camacho et al., 2009) command line tool. Hits were filtered by E-value less than 10^{-10}.

151

152 **Results**

153 *Transcriptome assembly and annotation*

154 Eight RNAseq libraries (two for each individual) were constructed and sequenced, yielding
155 between 63.9 x 10^6 and 139.5 x 10^6 paired reads per sample (Table 1). These reads were
156 assembled into contigs representing 171,051 putative transcripts deriving from 33,109
157 putative genes (Table 2). The frequency of the number of transcripts per gene is shown in
158 Fig. S2. Clustering using CD-HIT reduced the number of transcripts to 150,380. On average,
159 71% of the raw sequence reads aligned at least once to the reference transcriptome (Table
160 S1). After removing vector contamination, 147,397 transcripts remained.

161 The completeness of the transcriptome was assessed using BUSCO. Of the 978
162 single-copy orthologs that were searched for, 920 were found completely. Of these, 765
163 (78.2%) were found single-copy, 155 (15.8%) orthologs were found duplicated. A further
164 37 (3.8%) of the orthologs were found fragmented and 21 (2.2%) were not found in the
165 transcriptome.

166 A total of 111,416 (75.6%) transcripts were annotated by Trinotate. Protein
167 sequence comparison to the uniprot_sprot database yielded annotations for 89,386(60.6%)
168 transcripts, to the uniprot_uniref database for 87,045 (59.1%) transcripts and to the Pfam
169 database for 30,405 (20.6%) transcripts. After annotation, Trinotate assigned GO-terms to
170 19,658 genes, covering 26,039 transcripts (17.7%; Data S1).

171

172 *Differential expression*

Hierarchical clustering of the overall expression data clearly separated the mantle and foot tissue samples (Fig. 1). EdgeR identified 1,961 transcripts as upregulated and 1,260 as downregulated in the mantle relative to the foot (Fig. 2, Data S2).

Sequence polymorphisms

A total of 73,817 SNPs passed our filtering steps (Table S2). This included 12,273 synonymous and 12,451non-synonymous variants. The remaining 49,092 SNPs fell outside predicted open reading frames. A total of 569 SNPs were found in transcripts that were overexpressed in the mantle and showed phenotype-consistent allelic variation (Table 3). A total of 197 mantle-enriched transcripts contained at least one phenotype-consistent sequence variant. This set was subjected to more detailed annotation. We obtained database matches for 98 transcripts, of which 38 were functionally annotated (Table S3). Annotations that indicate putative functions related to shell formation are summarized in Table 4. Prominent among these annotations are sequences that are thought to play a role in the production of the nacreous layer in mollusc shells, including dermatopin and nacroperlin genes (marked in Table 4).

RAD-tags

A set of 12 transcripts had a match with at least one of the elongated tags that lie in close proximity to the supergene (Richards et al., 2013) (Table S4). None of these transcripts were found in our list of differentially expressed transcripts with phenotype-consistent variants. Eight of the twelve transcripts (matching two of the RAD tags closest to the supergene) had a blast hit to the nr and nt databases (Table S4, Data S3). All of these hits

196 were the *Helix pomatia* homolog of metallothionein. This same sequence was also found in
197 the variant analysis (six of 197 transcripts = 3%). None of the transcripts in these two sets
198 overlap. The percentage of metallothionein hits among the entire reference transcriptome
199 was 6,1% (2,506 of 40,748 transcripts), suggesting that this gene is not overrepresented in
200 our variant analysis.
201
202 **Discussion**
203 Our analysis identified a list of 300 candidate transcripts that were differentially expressed
204 in the shell-forming mantle tissue and contained SNP patterns that matched the shell
205 phenotypes. For most of these transcripts, it was impossible to infer their role in shell
206 formation as only ~20% of these genes were functionally annotated. Furthermore, the
207 supergene may consist mostly of regulatory genes without a previously identified role in
208 shell biosynthesis. However, two sets of transcripts could be putatively linked to shell or
209 pigment production.
210
211 The first set consists of transcripts involved in the synthesis of the nacreous layer in the
212 snail's shell. Mollusc shells consists of three layers: the outer prismatic layer, the inner
213 prismatic layer and the nacreous layer (Suzuki & Nagasawa, 2013). It is thought that
214 dermatopontin, a major shell matrix protein, is involved in the production of the nacreous
215 layer (Jiao et al., 2012). We found two hits to the *Euhadra herklotsi* ortholog of this gene.
216 Two other transcripts showed resemblance to Mucin 2, which is a gene that has a mollusc
217 homolog that is thought to be involved with production of the nacreous layer in molluscs
218 (Marin *et al.,* 2000). The mollusc variant of this gene is nacroperlin, which is found in shell

219 of Mediterranean mussels (Marin et al., 2000). The nacreous layer is the innermost layer of
220 the snail's shell and is therefore unlikely to directly affect pigmentation, however
221 differences in the nacreous layer may affect other shell traits that differ between the
222 morphs. Shell strength is known to differ between *C. nemoralis* colour morphs, with pink
223 shells stronger than yellow shells and banding stronger than no banding (Jiao et al., 2012;
224 Rosin et al., 2013).
225
226 The second set of transcripts consists of transcripts that produce metallothionein.
227 Metallothionein is a lightweight thiol-rich protein, the production of which is induced by
228 the presence of heavy metals such as zinc, copper or cadmium. This molecule inhibits the
229 production of melanin following oxidative stress (Sasaki et al., 2004). Melanin is a well-
230 known pigment that is found in many tissue types and often has a black or brown colour.
231 An inhibition of the production of melanin can possibly lead to a lack of pigmentation in the
232 tissue. This might contribute to the banding pattern or the ground colour of the shell.
233 Melanin pigments are produced in organelles called melanocytes, which contain a
234 subcellular zinc reservoir. This zinc can trigger a reaction with metallothionein to reduce
235 the production of melanin (Borovanský, 1994). The density of melanocytes in the snail
236 mantle was found to be correlated with darkness of the lip and possibly the banding
237 pattern on the shells (Emberton, 1963). The ground colour of the shell was not correlated
238 with the density of melanocytes. This suggests that the metallothionein transcripts we
239 identified could be involved in the production of the banding pattern and that they are less
240 likely to be involved in the ground colour.
241

242 The aim of this research was to find candidate genes underpinning the *Cepaea* shell colour
243 polymorphism. Due to the modest sample size, our power to detect differential expression
244 was limited. Furthermore, we found a relatively high ratio of synonymous to
245 nonsynonymous SNPs (close to 1:1), which was probably the result of over-prediction of
246 coding regions in partial transcripts and transcripts overlapping introns. This can result in
247 a higher number of predicted non-synonymous SNPS (Lopez-Maestre et al., 2016).
248 Nevertheless, we identified 300 candidates that showed mantle-specific expression and
249 phenotype-consistent SNP patterns. In addition to these, we found fifteen transcripts
250 matching RAD-tag sequences that are associated with the shell-colour supergene.
251 Functional annotation of these transcripts should be an excellent starting point for
252 elucidating the molecular underpinning on the *Cepaea* colour polymorphism.
253

254 **Acknowledgements**

255 We thank Heike Kappes for performing the snail dissections, Emile de Meijer and Henk
256 Buermans for RNA extraction and library preparation, and Peter Neleman, Mirna Baak and
257 Patrick Wijntjes for their earlier analysis of this dataset.
258

259 **Animal Ethics**

260 Not applicable
261

262 **DNA deposition**

The sequencing data has been deposited to NCBI's Sequence Read Archive (SRA) under accession SRP101411. The assembled transcriptome has been submitted to NCBI transcriptome shotgun assembly database (TSA) under BioProject No. PRJNA377398.

Supplemental Information

Figure S1 Snails used in this study.

Figure S2 Frequency distribution of the number of transcripts per gene.

Data S1 GO-annotation results

Data S2 Differential expression analysis results

Data S3 Hits and alignments of blasting the RAD-tags to the reference transcriptome.

References

Altschul SF., Gish W., Miller W., Myers EW., Lipman DJ. 1990. Basic local alignment search tool. *J. Mol. Biol.* 215:403–410. DOI: 10.1016/S0022-2836(05)80360-2.

Arnold RW. 1971. Heredity - Abstract of article: Cepaea nemorlis on the east sussex south Downs, and the nature of area effects. *Heredity* 26:277–298.

Borovanský J. 1994. Zinc in pigmented cells and structures, interactions and possible roles. *Sborník Lékařský* 95:309–320.

Cain AJ., Sheppard PM. 1950. Selection in the polymorphic land snail Cepaea nemoralis. *Heredity* 4:275–294.

Cain A., Sheppard P. 1952. The effects of natural selection on body colour in the land snail Cepaea nemoralis. *Heredity* 6:217–231.

Cain AJ., Sheppard PM. 1954. Natural Selection in Cepaea. *Genetics* 39:89–116.

286 Camacho C., Coulouris G., Avagyan V., Ma N., Papadopoulos J., Bealer K., Madden TL. 2009.
287 BLAST+: architecture and applications. *BMC Bioinformatics* 10:421. DOI:
288 10.1186/1471-2105-10-421.
289 Cameron RAD., Cook LM. 2012. Habitat and the shell polymorphism of Cepaea nemoralis
290 (L.): Interrogating the Evolution Megalab database. *Journal of Molluscan Studies*
291 78:179–184. DOI: 10.1093/mollus/eyr052.
292 Cingolani P., Platts A., Wang LL., Coon M., Nguyen T., Wang L., Land SJ., Ruden DM., Lu X.
293 2012. A program for annotating and predicting the effects of single nucleotide
294 polymorphisms, SnpEff: SNPs in the genome of Drosophila melanogaster strain
295 w1118 ; iso-2; iso-3. *Fly* 6:1–13.
296 Clarke B. 1962. Heredity - Abstract of article: Natural selection in mixed populations of two
297 polymorphic snails. *Heredity* 17:319–345.
298 Cook LM. 1998. A two-stage model for Cepaea polymorphism. *Philosophical Transactions of*
299 *the Royal Society B: Biological Sciences* 353:1577–1593. DOI: 10.1098/rstb.1998.0311.
300 Emberton LRB. 1963. Relationships Between Pigmentation of Shell and of Mantle in the
301 Snails Cepaea Nemoralis (l.) and Cepaea Hortensis (mull.). *Proceedings of the*
302 *Zoological Society of London* 140:273–293. DOI: 10.1111/j.1469-7998.1963.tb01864.x.
303 Fu L., Niu B., Zhu Z., Wu S., Li W. 2012. CD-HIT: Accelerated for clustering the next-
304 generation sequencing data. *Bioinformatics* 28:3150–3152. DOI:
305 10.1093/bioinformatics/bts565.
306 Grabherr MG., Haas BJ., Yassour M., Levin JZ., Thompson DA., Amit I., Adiconis X., Fan L.,
307 Raychowdhury R., Zeng Q., Chen Z., Mauceli E., Hacohen N., Gnirke A., Rhind N., di
308 Palma F., Birren BW., Nusbaum C., Lindblad-Toh K., Friedman N., Regev A. 2011.

309 Trinity: reconstructing a full-length transcriptome without a genome from RNA-Seq
310 data. *Nature biotechnology* 29:644–652. DOI: 10.1038/nbt.1883.
311 Greenwood J. 1974. Visual and other selection in Cepaea: A further example. *Heredity*
312 33:17–31.
313 Jiao Y., Wang H., Du X., Zhao X., Wang Q., Huang R., Deng Y. 2012. Dermatopontin, a shell
314 matrix protein gene from pearl oyster Pinctada martensii, participates in nacre
315 formation. *Biochemical and Biophysical Research Communications* 425:679–683. DOI:
316 10.1016/j.bbrc.2012.07.099.
317 Jones JS., Leith BH., Rawlings P. 1977. Polymorphism in Cepaea: a problem with too many
318 solutions? *Annual Review of Ecology and Systematics* 8:109–143.
319 Lamotte M. 1959. Polymorphism of Natural Populations of Cepaea nemoralis. *Cold Spring*
320 *Harbor Symposia on Quantitative Biology* 24:65–86. DOI:
321 10.1101/SQB.1959.024.01.009.
322 Langmead B., Salzberg SL. 2012. Fast gapped-read alignment with Bowtie 2. *Nature*
323 *methods* 9:357–9. DOI: 10.1038/nmeth.1923.
324 Lopez-Maestre, H., Brinza, L., Marchet, C., Kielbassa, J., Bastien, S., Boutigny, M., Monnin, D.,
325 Filali, A.E., Carareto, C.M., Vieira, C., et al. (2016). SNP calling from RNA-seq data
326 without a reference genome: identification, quantification, differential analysis and
327 impact on the protein sequence. Nucleic Acids Res. 44, e148–e148.
328 Mann K., Jackson DJ. 2014. Characterization of the pigmented shell-forming proteome of
329 the common grove snail Cepaea nemoralis. *BMC Genomics* 15:249. DOI: 10.1186/1471-
330 2164-15-249.
331 Marin F., Corstjens P., Gaulejac B de., Jong E de V-D., Westbroek P. 2000. Mucins and

molluscan calcification. Molecular characterization of mucoperlin, a novel mucin-like protein from the nacreous shell layer of the fan mussel Pinna nobilis (Bivalvia, pteriomorphia). *Journal of Biological Chemistry* 275:20667–20675. DOI: 10.1074/jbc.M003006200.

McKenna A., Hanna M., Banks E., Sivachenko A., Cibulskis K., Kernytsky A., Garimella K., Altshuler D., Gabriel S., Daly M., DePristo M a. 2010. The Genome Analysis Toolkit: a MapReduce framework for analyzing next-generation DNA sequencing data. *Genome research* 20:1297–303. DOI: 10.1101/gr.107524.110.

Murray J. 1963. The Inheritance of Some Characters in Cepaea Hortensis and Cepaea Nemoralis (Gastropoda). *Genetics* 48:605–615.

Richards PM., Liu MM., Lowe N., Davey JW., Blaxter ML., Davison A. 2013. RAD-Seq derived markers flank the shell colour and banding loci of the Cepaea nemoralis supergene. *Molecular Ecology* 22:3077–3089. DOI: 10.1111/mec.12262.

Roberts A., Pachter L. 2013. Streaming fragment assignment for real-time analysis of sequencing experiments. *Nature Methods* 10:71–73. DOI: 10.1038/nmeth.2251.

Robinson MD., McCarthy DJ., Smyth GK. 2010. edgeR: a Bioconductor package for differential expression analysis of digital gene expression data. *Bioinformatics (Oxford, England)* 26:139–140. DOI: 10.1093/bioinformatics/btp616.

Rosin ZM., Kobak J., Lesicki A., Tryjanowski P. 2013. Differential shell strength of Cepaea nemoralis colour morphs--implications for their anti-predator defence. *Die Naturwissenschaften* 100:843–851. DOI: 10.1007/s00114-013-1084-8.

Sasaki M., Kizawa K., Igarashi S., Horikoshi T., Uchiwa H., Miyachi Y. 2004. Suppression of melanogenesis by induction of endogenous intracellular metallothionein in human

355 melanocytes. *Experimental Dermatology* 13:465–471. DOI: 10.1111/j.0906-
356 6705.2004.00204.x.
357 Salazar-Jaramillo L., Jalvingh KM., de Haan A., Kraaijeveld K., Buermans H., Wertheim B.
358 2017. Inter- and intra-species variation in genome-wide gene expression of Drosophila
359 in response to parasitoid wasp attack. *BMC Genomics* 18:331. DOI: 10.1186/s12864-
360 017-3697-3.
361 Schilthuizen M. 2013. Rapid, habitat-related evolution of land snail colour morphs on
362 reclaimed land. *Heredity* 110:247–52. DOI: 10.1038/hdy.2012.74.
363 Schwander T., Libbrecht R., Keller L. 2014. Supergenes and complex phenotypes. *Current*
364 *Biology* 24:R288–R294. DOI: 10.1016/j.cub.2014.01.056.
365 Silvertown J., Cook L., Cameron R., Dodd M., McConway K., Worthington J., Skelton P., Anton
366 C., Bossdorf O., Baur B., Schilthuizen M., Fontaine B., Sattmann H., Bertorelle G., Correia
367 M., Oliveira C., Pokryszko B., Ozgo M., Stalažs A., Gill E., Rammul Ü., Sólymos P., Féher
368 Z., Juan X. 2011. Citizen science reveals unexpected continental-scale evolutionary
369 change in a model organism. *PLoS ONE* 6. DOI: 10.1371/journal.pone.0018927.
370 Simao FA., Waterhouse RM., Ioannidis P., Kriventseva E V., Zdobnov EM. 2015. BUSCO:
371 Assessing genome assembly and annotation completeness with single-copy orthologs.
372 *Bioinformatics* 31:3210–3212. DOI: 10.1093/bioinformatics/btv351.
373 Suzuki M., Nagasawa H. 2013. Mollusk shell structures and their formation mechanism.
374 *Canadian Journal of Zoology* 91:349–366. DOI: 10.1139/cjz-2012-0333.
375 Worthington JP., Silvertown J., Cook L., Cameron R., Dodd M., Greenwood RM., McConway
376 K., Skelton P. 2012. Evolution MegaLab: a case study in citizen science methods.
377 *Methods in Ecology and Evolution* 3:303–309. DOI: 10.1111/j.2041-

378 210X.2011.00164.x.

379

380

381

Table 1 Overview of number of reads and GC content per sample and tissue.

Sample	Individual	Tissue	Number of reads	Number of bases	GC Content
11	1	Foot	71,694,188	6,273,241,450	44%
12	1	Mantle	71,670,338	6,271,154,575	46%
13	2	Foot	77,053,092	6,742,145,550	43%
14	2	Mantle	66,729,632	5,838,842,800	46%
15	3	Foot	63,903,422	5,591,549,425	46%
16	3	Mantle	69,572,264	6,087,573,100	49%
17	4	Foot	121,731,962	10,651,546,675	46%
18	4	Mantle	139,455,234	12,202,332,975	49%

Table 2 Statistics of the transcriptome assembly.

Statistic	Number	Number after filtering
Number of contigs	171,051	147,411
Average contig length	847.86 bp	783.47 bp
Median contig length	537 bp	515 bp
Number of genes	33,109	25,334
N50	1,111	968
GC Content	42.20%	42%
Total bases	145,027,740	115,481,543

Table 3 Numbers of SNPs that were homozygous in the yellow snails and the number of transcripts these were found in. These are further broken down into sets that showed allelic patterns that were consistent with the shell phenotypes of the sampled snails, differentially expressed in mantle tissue or both.

Property	Number of SNPS	Number of transcripts
Total number	73,817	17,499
Consistent	5,776	2,592
Differentially Expressed	4,992	817
Differentially expressed and consistent	569	197

403
404
405
406
407 **Table 4** The most informative annotations from Supplementary Table S3. Transcripts with
408 putative function in nacre and shell production are marked in italics.
409
410

Contig name	Functional annotation	Effect
c280576_g1_i1	*Biomphalaria glabrata* glycine and methionine-rich –like	synonymous_variant
c280925_g1_i2	*Parasteatoda tepidariorum* keratin-associated 6-2-like	synonymous_variant
c350256_g1_i1	*Anas platyrhynchos* BPI fold-containing family B member 3	synonymous_variant
c368572_g1_i1	*Aplysia californica* epithelial splicing regulatory 1-like	synonymous_variant
c369765_g4_i2	*Biomphalaria glabrata* ferric-chelate reductase 1-like	synonymous_variant
c371799_g2_i1	*Biomphalaria glabrata* sushi, von Willebrand factor type A, EGF and pentraxin domain-containing 1-like	synonymous_variant
c264073_g1_i1	*Camelus bactrianus mucin-2-like*	*frameshift_variant & stop_gained inframe_insertion*
c366293_g1_i1	*Biomphalaria glabrata mucin-2-like*	*missense_variant*
c321814_g1_i1	*Euhadra herklotsi mRNA for Dermatopontin1*	*intergenic_region*
c355427_g1_i1	*Euhadra herklotsi mRNA for Dermatopontin1*	*stop_gained missense_variant*

411

412 **Figure legends**

413 **Figure 1** Overall gene expression differences according to tissue and individual snail.

414 **Figure 2** Scatterplot (A):log counts versus log fold change and volcano plot (B): log fold

415 change versus statistical significance, for differential expression in mantle tissue versus the

416 foot tissue, obtained using EdgeR. Transcripts marked in red were considered differentially

417 expressed.

418

419

420

421 Figure 1

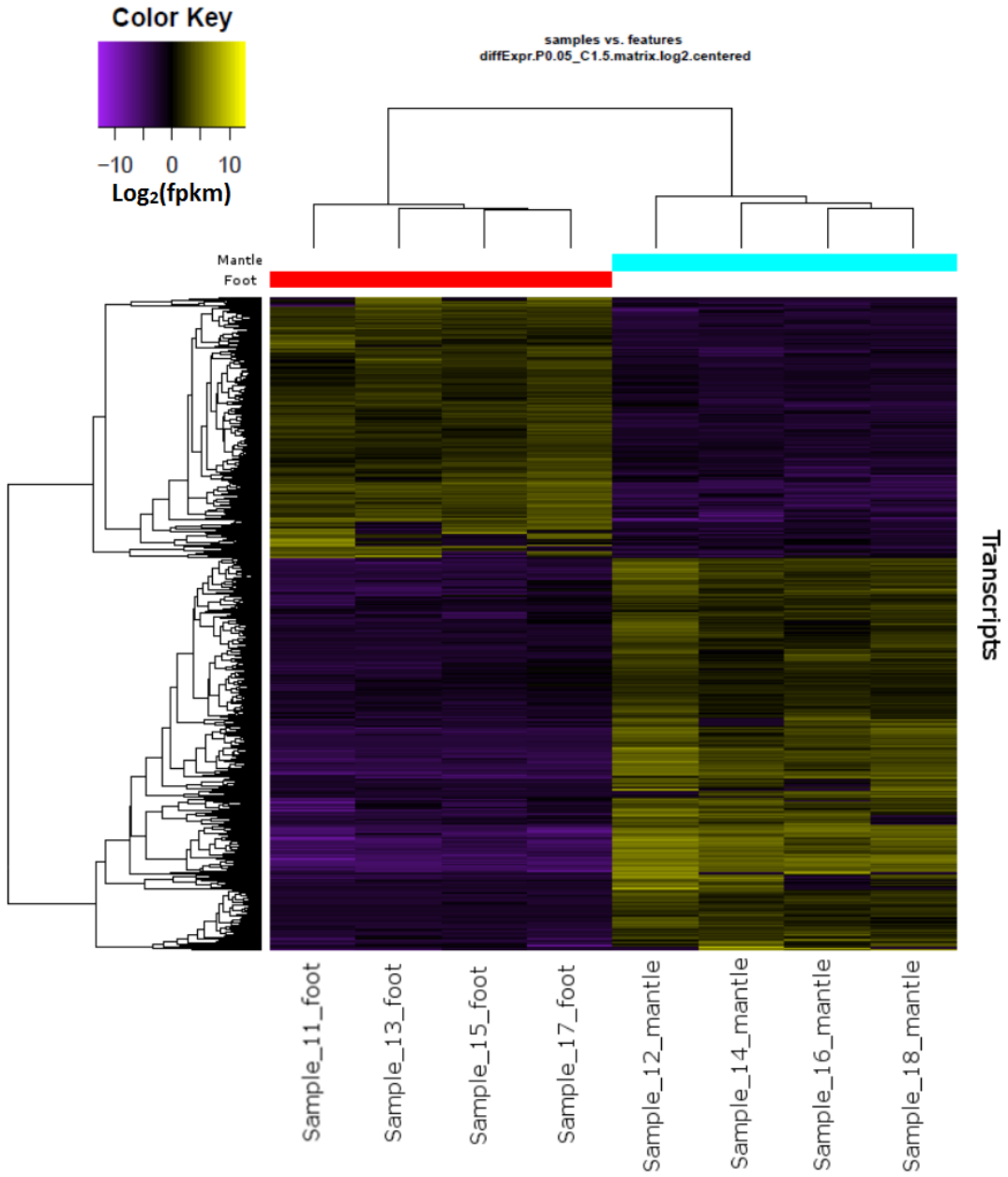

422

423

424

425 Figure 2

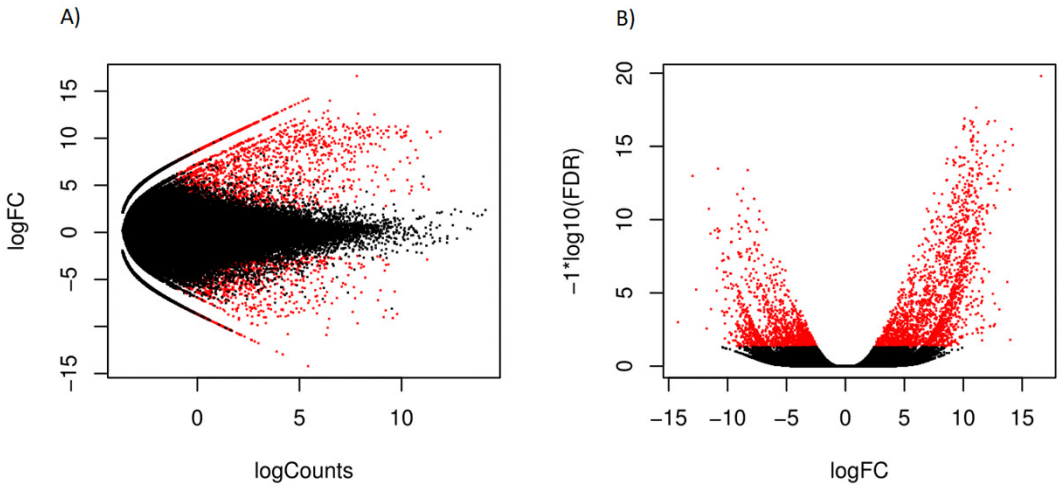

426

427

428